

Transport and Coulomb drag for two interacting carbon nanotubes

A. Komnik and R. Egger

Fakultät für Physik, Albert-Ludwigs-Universität, D-79104 Freiburg, Germany

Date: October 28, 2018

Abstract. We study nonlinear transport for two coupled one-dimensional quantum wires or carbon nanotubes described by Luttinger liquid theory. Transport properties are shown to crucially depend on the contact length L_c . For a special interaction strength, the problem can be solved analytically for arbitrary L_c . For point-like contacts and strong interactions, a qualitatively different picture compared to a Fermi liquid emerges, characterized by zero-bias anomalies and strong dependence on the applied cross voltage. In addition, pronounced Coulomb drag phenomena are important for extended contacts.

PACS. 71.10.Pm , 72.10.-d, 72.80.Rj

1 Introduction

Transport in interacting one-dimensional (1D) quantum wires (QW) has attracted ever-increasing attention over the past decade. This interest was sparked mainly by the discovery of novel 1D materials besides standard (semiconductor or organic chain molecule) systems, such as edge states in fractional quantum Hall bars or carbon nanotubes. Furthermore, 1D QWs are predicted to behave as a Luttinger liquid (LL) due to electron-electron interactions [1]. Recent nonlinear transport experiments [2] for individual nanotubes have indeed demonstrated impressive agreement with the LL theory of nanotubes [3]. In these experiments, transport was limited either by the contact resistance to the leads, or by a tunnel junction (“topological kink”) within the nanotube. In both cases, the observed power laws in the (nonlinear) conductance have allowed for a consistent explanation in terms of LL theory.

Different transport experiments built up of at least two nanotubes can reveal even more dramatic deviations from Fermi liquid transport. The theoretical predictions of Ref. [4] for crossed nanotubes (which are coupled in a pointlike way) were recently observed experimentally by Kim *et al.* [5]. For longer contacts between the nanotubes, Coulomb drag [6] is expected to play an important role in addition to the crossed nanotube scenario. Coulomb drag can be very pronounced in one dimension and leads to quite rich physics. In this paper, we study in detail two nanotubes arranged parallel to or crossing each other, and briefly discuss more complex setups. Notably, such experiments are feasible using present-day technology [5, 7].

The main part of the paper focuses on the schematic geometry shown in Figure 1, where transport through two

clean (ballistic) nanotubes biased by voltages $U_{1,2}$ is studied. The nanotubes are brought to contact by crossing them under an angle Ω . By varying this angle, the effective contact length L_c can be changed. We shall address the crossover from a point-like crossing, where $L_c \approx a$ with the lattice spacing a , to an extended coupling, where $a \ll L_c \leq L$ with the tube length L . Besides our previous paper [4], theoretical predictions for transport in such a geometry have been given by other authors [8, 9, 10, 11]. Their results were largely obtained in the linear regime, or focus on either very small or very large L_c . In this paper, we cover the full crossover from a point-like to an extended contact, and explicitly compute *nonlinear* current-voltage relations. For simplicity, we consider the same interaction strength parameter g and Fermi velocity v_F for both QWs. The LL parameter g equals unity for a Fermi gas, and becomes smaller for strong repulsive interactions. Provided one works on an insulating substrate, the LL parameter has only a weak logarithmic dependence on the tube length L , and the experimentally observed value $g \approx 0.25$ [2, 3, 5] indicates strong non-Fermi liquid behavior.

For repulsive interactions ($g < 1$), the most important coupling between the two nanotubes is of electrostatic origin [4]. It is responsible for the most relevant operator under the renormalization group (RG), and can cause perfect Coulomb drag at low temperatures. In addition, as indicated by the data of Ref. [7], electron tunneling between the QWs can be important. Provided one has sufficiently strong interactions, tunneling into a LL is *irrelevant* in the RG sense. In that case, one can treat it perturbatively, at least for not exceedingly large tunneling amplitude. Notice that otherwise our assumption of clean wires breaks down in any case, since good mechanical contact of the QWs indicates impurity formation within each QW.

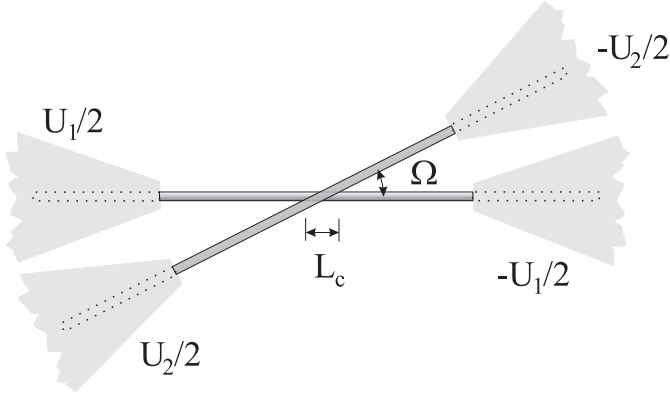


Fig. 1. Two crossed nanotubes in contact to reservoirs for applied voltage U_1 and U_2 , respectively (schematic view). Different crossing angles Ω imply different effective contact lengths L_c .

The outline of our paper is as follows. In Sec. 2, we briefly review the LL concept and discuss how the theory can incorporate adiabatically coupled voltage reservoirs in terms of Sommerfeld-like radiative boundary conditions [12]. Sec. 3 presents a detailed discussion of transport for the setup in Fig. 1 under the assumption of negligible tunneling. In particular, for the special interaction strength $g = 1/2$, the full temperature-dependent transport problem is solved for arbitrary contact length L_c . The role of adiabaticity of the contacts to the reservoirs for the described effects is addressed in Sec. 4, where we study weakly contacted reservoirs in the tunneling limit. In Sec. 5, effects of inter-wire tunneling are discussed, and in Sec. 6 some conclusions and possible applications are outlined.

For clarity, we focus on spinless single-channel QWs. The modifications arising for spin-1/2 electrons or carbon nanotubes are then straightforward. In addition, the relevant energy scale is supposed to exceed v_F/L , so that we can effectively put $L \rightarrow \infty$. Below we put $\hbar = e = k_B = 1$ and $v = v_F/g = 1$.

2 Model

The LL concept for 1D metals is most transparent in the bosonization representation [1]. The electron field operator is written as superposition of left- and right-moving ($p = R/L = \pm$) fermions $\psi_{p\alpha}(x)$ for QW $\alpha = 1, 2$. The latter are expressed in terms of canonically conjugate bosonic fields $\theta_\alpha(x)$ and $\phi_\alpha(x)$,

$$\psi_{p\alpha}(x) \sim (2\pi a)^{-1/2} \exp[-ipk_{F\alpha}x] \times \exp[-ip(\pi g)^{1/2}\theta_\alpha(x) - i(\pi/g)^{1/2}\phi_\alpha(x)], \quad (1)$$

where a is a lattice constant. The Fermi momentum $k_{F\alpha}$ in the two QWs can be made different by uniformly shifting the chemical potentials of both reservoirs attached to one wire. The $k_{F\alpha}$ are defined such that the chemical potentials are $\pm U_{1,2}/2$ as indicated in Figure 1. Using Eq. (1),

the density operator $\rho_\alpha(x)$ is

$$\rho_\alpha = (g/\pi)^{1/2} \partial_x \theta_\alpha + \frac{k_{F\alpha}}{\pi} \sin \left[2k_{F\alpha}x + \sqrt{4\pi g} \theta_\alpha \right]. \quad (2)$$

The uncoupled clean QWs correspond to the standard LL Hamiltonian,

$$H_0 = \sum_\alpha \frac{1}{2} \int dx \left[(\partial_x \phi_\alpha)^2 + (\partial_x \theta_\alpha)^2 \right]. \quad (3)$$

Let us next address how the coupling of each wire to the voltage reservoirs can be taken into account. For adiabatic coupling, the electron densities near the end of the QW obey the radiative boundary conditions [12]

$$\frac{g^{-2} \pm 1}{2} \rho_{R\alpha}(\mp L/2) + \frac{g^{-2} \mp 1}{2} \rho_{L\alpha}(\mp L/2) = \pm \frac{U_\alpha}{4\pi g}, \quad (4)$$

where the $p = R/L = \pm$ moving densities in wire α are

$$\rho_{p\alpha}(x) = (4\pi g)^{-1/2} \partial_x [g\theta_\alpha + p\phi_\alpha]. \quad (5)$$

These boundary conditions need to be enforced for the stationary expectation values of the densities $\rho_{p\alpha}$ in the QW near the respective contact to the leads. They hold for arbitrary impurity scattering within each wire and therefore also in the presence of coupling between the two wires.

In the absence of inter-wire tunneling, the charge current

$$I_\alpha(x) = e(g/\pi)^{1/2} \partial_t \theta_\alpha(x) \quad (6)$$

is conserved and independent of x . In the presence of tunneling, however, we need to distinguish $I_\alpha(x < -L_c/2)$ and $I_\alpha(x > L_c/2)$. Postponing the discussion of inter-wire tunneling to Sec. 5, the conductance of each (impurity-free) QW is thus $G_0 = e^2/h$ in the absence of *electrostatic* inter-wire coupling. The latter then implies a reduction of the conductance

$$G_\alpha = I_\alpha/U_\alpha, \quad (7)$$

since the transport-carrying density waves drag each other, which makes them “heavier.” For low energy scales, the electrostatic coupling can be expressed as a *local* product of densities in the two wires. To justify the locality of inter-wire interactions, one can employ the same reasoning as for the locality of the intra-wire interaction [1]. Neglecting momentum-non-conserving terms, we obtain

$$\begin{aligned} H_1 &= V_1 \int dx \zeta(x) \rho_1(x) \rho_2(x) \\ &= V_{1a} \int dx \zeta(x) \partial_x \theta_1 \partial_x \theta_2 \\ &\quad + V_{1b} \int dx \zeta(x) \sin \left[2k_{F1}x + \sqrt{4\pi g} \theta_1(x) \right] \\ &\quad \times \sin \left[2k_{F2}x + \sqrt{4\pi g} \theta_2(x) \right], \end{aligned} \quad (8)$$

where $V_{1a} = gV_1/\pi$ and $V_{1b} = V_1 k_{F1} k_{F2} / \pi^2$. The function $\zeta(x)$ specifies the spatial dependence of the inter-wire coupling, and for practical purposes, we consider $\zeta(x) = 1$ for $|x| \leq L_c/2$ and zero otherwise,

$$\zeta(x) = [\Theta(x + L_c/2) - \Theta(x - L_c/2)]. \quad (9)$$

In addition, *tunneling* leads to

$$H_2 = V_2 \int dx \zeta(x) \sum_{pp'} \psi_{p1}^\dagger(x) \psi_{p'2}(x) + \text{h.c.}, \quad (10)$$

describing electron transfer between the QWs. The bosonized form of H_2 can be found in Ref. [4]. We shall turn to a discussion of tunneling in Sec. 5. Josephson-type couplings [13] are irrelevant for $g < 1$ and hence will be ignored in the following.

3 Electrostatically coupled nanotubes

In this section, we assume that tunneling can be neglected, and consider a system described by the Hamiltonian $H = H_0 + H_1$ under the boundary conditions (4). Below we separately discuss three cases, namely (a) a strictly local contact with $L_c \rightarrow 0$, (b) a short but finite contact length $L_c \approx a$, and (c) for the special interaction strength $g = 1/2$, we present an analytical solution valid for arbitrarily long contacts. Of particular interest is the *differential conductance matrix*,

$$G_{\alpha\alpha'} = \partial I_\alpha / \partial U_{\alpha'}. \quad (11)$$

The off-diagonal conductance G_{12} (or G_{21}), the so-called “transconductance”, is the appropriate quantity measuring Coulomb drag [6]. For $U_1 = U_2 = 0$, the matrix $G_{\alpha\alpha'}$ describes the linear conductances. Generally, the diagonal conductance $G_{\alpha\alpha}$ and the conductance G_α defined in Eq. (7) show qualitatively the same behavior.

3.1 Strictly local contact

Let us start with an ideal point-like contact, where from Eq. (9), we get for $L_c \rightarrow 0$ the result $\zeta(x) = L_c \delta(x)$. In that case, tunneling is always irrelevant for $g < 1$, and the only *relevant* coupling corresponds to the scaling field V_{1b} in Eq. (8), provided $g < 1/2$. For $g > 1/2$, the effects of tunneling (V_2) and of the electrostatic coupling (V_{1b}) can both be treated perturbatively. We shall therefore focus on the most interesting strong-interaction region $g < 1/2$ in this subsection, and omit the irrelevant perturbation V_{1a} as well as tunneling (V_2). Introducing symmetric and antisymmetric fields [4],

$$\begin{aligned} \theta_\pm(x) &= [\theta_1(x) \pm \theta_2(x)]/\sqrt{2}, \\ \phi_\pm(x) &= [\phi_1(x) \pm \phi_2(x)]/\sqrt{2}, \end{aligned} \quad (12)$$

the Hamiltonian decouples, $H = H_+ + H_-$, with

$$\begin{aligned} H_\pm &= \frac{1}{2} \int dx [(\partial_x \phi_\pm)^2 + (\partial_x \theta_\pm)^2] \\ &\pm (L_c V_{1b}/2) \cos[\sqrt{8\pi g} \theta_\pm(0)]. \end{aligned} \quad (13)$$

An effective coupling strength is defined as

$$T_B = (c_g/a)[aL_c V_{1b}]^{1/(1-2g)}, \quad (14)$$

where c_g is a numerical constant of order unity [14,15]. The boundary conditions (4) also decouple in the symmetric/antisymmetric ($r = \pm$) channels. Effective right- and left-moving ($p = R/L = \pm$) densities $\bar{\rho}_{pr}(x)$ for these channels can be defined in analogy to Eq. (5). The new densities again obey the boundary conditions (4), but with the effective voltages

$$U_{1,2} \rightarrow U_{r=\pm} = (U_1 \pm U_2)/\sqrt{2}. \quad (15)$$

It is also useful to define the effective current \bar{I}_r in channel $r = \pm$, see Eq. (6). The current in QW $\alpha = 1, 2$ is then given by $I_\alpha = (\bar{I}_+ \pm \bar{I}_-)/\sqrt{2}$.

Notably, the full nonlinear correlated transport problem of crossed LLs therefore completely decouples into two effective single-impurity problems $r = \pm$ characterized by effective impurity strength $\pm T_B$, applied voltage $(U_1 \pm U_2)/\sqrt{2}$, and interaction strength $2g$. This single-impurity problem has been studied in detail, e.g. by Kane and Fisher [14], and the exact solution for arbitrary interaction strength has been given in Ref. [15] by combining Eq. (4) and powerful methods from boundary conformal field theory. This solution can then be immediately applied to the crossed LL transport problem. Below we discuss the salient features for the special case $g = 1/4$. These features are characteristic for the strong-interaction regime $g < 1/2$. For weak interactions, $g > 1/2$, all interwire couplings may be treated in perturbation theory, and results can be found, e.g. in Ref. [8].

The currents through QW $\alpha = 1, 2$ are

$$I_\alpha = (e^2/h)[U_\alpha - (V_+ \pm V_-)/\sqrt{2}], \quad (16)$$

where V_\pm obeys the self-consistency relation [15]

$$V_\pm = 2T_B \text{Im} \Psi \left(\frac{1}{2} + \frac{T_B + i(U_\pm - V_\pm/2)}{2\pi T} \right), \quad (17)$$

with the digamma function Ψ . Similar but more complicated self-consistency equations need to be solved for $g \neq 1/4$. From Eq. (16), one can verify that the conductance matrix (11) fulfills the bounds

$$0 \leq G_{11}/G_0 \leq 1, \quad -1/2 \leq G_{12}/G_0 \leq 1/2, \quad (18)$$

with $G_0 = e^2/h$. The current-voltage relation (16) or, equivalently, the nonlinear conductances $G_{\alpha\alpha'}$ are very different from the corresponding results for Fermi liquids [6]. The correlation effects are most pronounced for $T = 0$ [4], where perfect zero-bias anomalies, a strong dependence of G_{11} on the applied cross voltage U_2 , and minima in G_{11} for $|U_1| = |U_2|$ are predicted. Such effects are distinct and dramatic signatures of correlations in a LL, and have found evidence in recent experiments on crossed multi-wall nanotubes [5]. Note that for a Fermi liquid, G_{11} would neither depend on U_1 nor on U_2 . Thermal fluctuations tend to smear out these phenomena, see Fig. 2, but they remain clearly discernible.

In the linear transport regime, $|U_{1,2}| \ll T$, by Taylor expanding Eq. (17) in the small parameter $(U_1 \pm U_2)/T$,

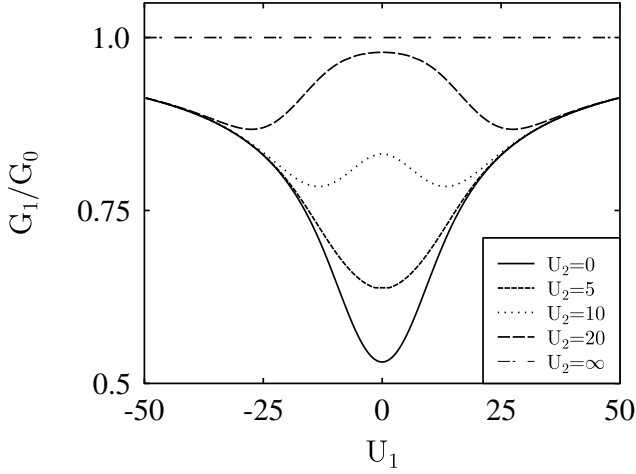


Fig. 2. Nonlinear conductance $G_1(U_1, U_2) = I_1/U_1$ for $g = 1/4$, $T = 2$ and various U_2 . Units are chosen such that $T_B = 1$ and $G_0 = e^2/h$.

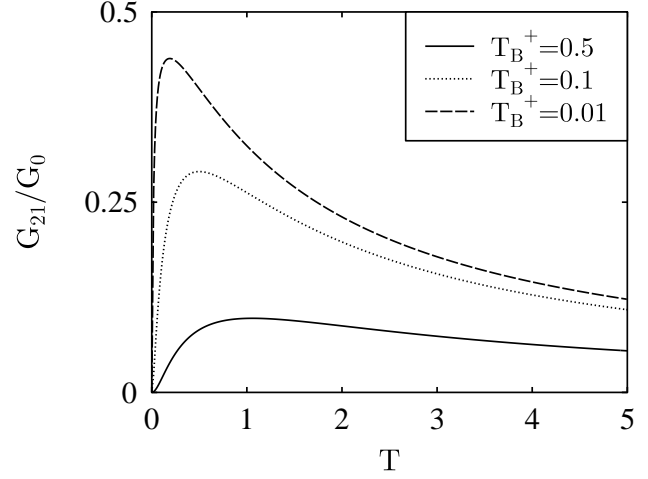


Fig. 3. Temperature dependence of the linear transconductance for a short contact length at $g = 1/4$. We put $T_B^- = 1$. Note that $G_{21} \rightarrow 0$ for $T \rightarrow 0$.

we find for $g = 1/4$ the voltage-independent linear conductance,

$$G_1/G_0 = \frac{1 - c\Psi'(\frac{1}{2} + c)}{1 + c\Psi'(\frac{1}{2} + c)}, \quad c = T_B/2\pi T. \quad (19)$$

More interesting is the *transconductance*, which reads to leading order in $(U_1 \pm U_2)/T$:

$$G_{12}/G_0 = \frac{U_1 U_2}{T_B^2} c^3 \Psi'''(\frac{1}{2} + c). \quad (20)$$

Clearly, for very small applied voltages (either U_1 or U_2 approaching zero), the transconductance vanishes. As shown in Sec. 3.2, the vanishing linear transconductance is a general consequence of the point-like nature assumed for the contact. For an extended contact, the linear transconductance need not vanish. For low temperatures, $|U_{1,2}| \ll T \ll T_B$, Eq. (20) gives $G_{12}/G_0 \simeq 2U_1 U_2 / T_B^2$, while in the high-temperature limit, $T \gg T_B$, we find $G_{12}/G_0 \simeq \pi U_1 U_2 T_B / 8T^3$.

Finally, for very strong interactions, $g \leq 0.1$, bistability effects were reported in Ref. [15]. As these phenomena require spinless electrons and cannot be observed in nanotubes, however, we do not further discuss them here. Based on the mapping of the transport problem of crossed LLs to two decoupled single-impurity problems, it is nevertheless straightforward to obtain the conductance matrix in closed form in the bistability regime.

3.2 Short contact

Next we turn to a short but nonlocal coupling, where L_c is of the order of a few lattice spacings a . For short contact length, the bosonic fields can be expanded in powers of x around the center of the coupling region, $x = 0$. The subsequent RG analysis shows that the only relevant coupling

term is still due to the scaling field V_{1b} , and one arrives again at the Hamiltonian (13). The only difference is the replacement $V_{1b} \rightarrow V_{1b}^\pm$ with

$$L_c V_{1b}^\pm = V_{1b} \int dx \zeta(x) \cos[2(k_{F1} \pm k_{F2})x], \quad (21)$$

leading to couplings T_B^\pm as in Eq. (14). For large L_c , $T_B^+ \ll T_B^-$ due to the oscillatory integrand. The resulting physics is similar to the point-like case of Sec. 3.1, but in addition exhibits linear *Coulomb drag* [8, 9]. Notably, we can exploit the exact solution of Ref. [15] for the single-impurity problem to solve this problem too.

In the remainder of this subsection, we again focus on the case of $g = 1/4$ where the algebra becomes quite simple. In particular, one has to solve the self-consistency equations (17) with $T_B \rightarrow T_B^\pm$. For clarity, we consider the special case $U_2 = 0$, and compute the transconductance G_{21} defined in Eq. (11). Notably, even though $U_2 = 0$, the current I_2 and hence G_{21} can be finite (Coulomb drag). The transconductance follows from

$$G_{21}(U_1, T)/G_0 = \frac{1}{\sqrt{2}} \frac{\partial}{\partial U_1} (V_- - V_+), \quad (22)$$

where the V_\pm are determined as the $U_2 = 0$ solutions of Eq. (17) with $T_B \rightarrow T_B^\pm$.

The *linear transconductance* at $T > 0$ can now be finite due to the nonlocality of the contact [8]. We find

$$G_{21}/G_0 = \frac{1}{2} \sum_{\pm} \pm \frac{1 - c_{\pm} \Psi'(\frac{1}{2} + c_{\pm})}{1 + c_{\pm} \Psi'(\frac{1}{2} + c_{\pm})}, \quad (23)$$

where $c_{\pm} \equiv T_B^\pm / 2\pi T$. The temperature dependence of the $g = 1/4$ linear transconductance (23) is shown in Fig. 3. We observe that for a long contact, $T_B^+ \ll T_B^-$, the perfectly quantized transconductance $e^2/2h$ is approached at

low but finite temperature. This is the *absolute drag effect* reported by Nazarov and Averin [9] for a long extended contact. Equation (23) then describes how the absolute drag effect is thermally destroyed at high temperatures.

However, as $T \rightarrow 0$, the linear transconductance *vanishes* throughout the strong interaction regime $g < 1/2$. (This is an artefact of the locality assumption and will not be true for extended contacts, see below.) In the zero-temperature limit, one can obtain the nonlinear $g = 1/4$ transconductance for $|U_1| \ll T_B^\pm$ and $U_2 = 0$ from Eqs. (22) and (17),

$$G_{21}/G_0 = (U_1/4)^2[(T_B^+)^{-2} - (T_B^-)^{-2}] + O([U_1/T_B^+]^4). \quad (24)$$

Finally, let us address the role of a difference in the Fermi momenta, $\delta k_F = k_{F1} - k_{F2}$, which could experimentally be tuned by varying the mean chemical potential in one QW relative to the other. In the absence of electron tunneling between the QWs, the nonlinear conductance matrix $G_{\alpha\alpha'}(U_1, U_2)$ for a short contact does only depend on δk_F via the T_B^\pm following from Eq. (21). In fact, for a strictly local contact ($T_B^\pm = T_B$), there is no dependence on δk_F at all unless there is tunneling. As discussed in Sec. 5, this effect can be used to experimentally disentangle the effects of tunneling and electrostatic coupling.

3.3 Arbitrary contact length

Next we study an arbitrarily long contact, where L_c can even approach the system length L . Here tunneling can be a relevant perturbation under the RG transformation, provided the interaction is not too strong. Following the analysis of Refs. [16,17], for $g > g' = \sqrt{2} - 1 \simeq 0.414$, tunneling is relevant. In fact, for $g > g'' = 1/\sqrt{3} \simeq 0.577$, tunneling (V_2) is even more relevant than the electrostatic coupling V_{1b} . In this regime, one should then first treat the tunneling. Below we focus on the strong-interaction case, $g < g''$. For $g' < g < g''$, the main effect of tunneling is a renormalization of the electrostatic coupling [17]. In the following we assume that V_{1b} contains this renormalization and then omit the scaling field V_2 . Since for a short contact, tunneling is always irrelevant, such a reasoning can be applied for arbitrary L_c in the regime $g < g''$, in particular for the case $g = 1/2$ investigated below.

Taking into account the V_{1a} operator in the bulk (i.e., for $L_c = L$) causes a renormalization of the interaction constants, thereby splitting them [10],

$$g \rightarrow g_\pm = \frac{g}{\sqrt{1 \pm gV_{1a}}}. \quad (25)$$

For $L_c \ll L$, however, the scaling field V_{1a} is *irrelevant*. Below we shall neglect the weak splitting (25). Following our analysis, this could only create a problem for very long contacts, $L_c \approx L$. The case $g = 1/2$ then permits a full solution of this transport problem for arbitrary L_c . The resulting effective Hamiltonian is

$$H = H_0 + V_{1b} \int dx \zeta(x) \sin \left[2k_{F1}x + \sqrt{2\pi} \theta_1(x) \right] \times \sin \left[-2k_{F2}x + \sqrt{2\pi} \theta_2(-x) \right], \quad (26)$$

where the spatial coordinate along QW $\alpha = 2$ has been changed to $-x$. As we shall see later, this mirroring of the axis is crucial to ensure correct anticommutation relations between new fermionic fields. Expanding the product of sin terms, cos functions of the sum and the difference of the fields θ_α emerge. In Ref. [9], only the difference term was kept, since the other term is highly oscillatory for long contacts and does not contribute for $L_c \gg a$. However, a proper description of the crossover from a short to a long contact requires to consider the full coupling (26). Below we take Eq. (9) for $\zeta(x)$.

3.3.1 Refermionization

Remarkably, the transport problem posed by Eqs. (26) and (4) can be solved exactly for arbitrary L_c by refermionization. Switching to the chiral fields,

$$\varphi_{R,L}^\alpha = \sqrt{\pi}(\phi_\alpha \pm \theta_\alpha), \quad (27)$$

we obtain with $\delta k_F = k_{F1} - k_{F2}$ and $2k_F = k_{F1} + k_{F2}$

$$H = \frac{1}{8\pi} \sum_{\alpha=1,2} \int dx [(\partial_x \varphi_L^\alpha)^2 + (\partial_x \varphi_R^\alpha)^2] - V_{1b} \int dx \zeta(x) \left\{ \sum_{p=\pm} e^{ip2\delta k_F x} e^{ip(\varphi_R^1(x) - \varphi_L^2(-x))/\sqrt{2}} \times e^{-ip(\varphi_L^1(x) - \varphi_R^2(-x))/\sqrt{2}} - e^{ip[4k_F x + (\varphi_R^1(x) + \varphi_L^2(-x))/\sqrt{2}]} \times e^{-ip(\varphi_L^1(x) + \varphi_R^2(-x))/\sqrt{2}} \right\}.$$

We then employ the slightly modified refermionization transformation of Luther and Emery [18],

$$\Psi_{1,2}(x) = \frac{\eta_{1,2}}{\sqrt{2\pi a}} e^{i2k_{F1}x + i(\varphi_R^1(x) \mp \varphi_L^2(-x))/\sqrt{2}}, \quad (28)$$

$$\Psi_{3,4}(x) = \frac{\eta_{3,4}}{\sqrt{2\pi a}} e^{\pm i2k_{F2}x \mp i(\varphi_R^2(-x) \mp \varphi_L^1(x))/\sqrt{2}}.$$

Special Majorana fermions η_i ensure the correct anticommutation relations between new operators, see Ref. [3]. However, all chemical potentials of the new particles can be incorporated into the refermionized Hamiltonian ($\lambda = 2\pi a V_{1b}$)

$$H = - \int dx \left\{ \sum_{j=1,2} \Psi_j^\dagger(x) (i\partial_x + 2k_{F1}) \Psi_j(x) - \sum_{j=3,4} \Psi_j^\dagger(x) (i\partial_x \mp 2k_{F2}) \Psi_j(x) \right\} + i\lambda \int dx \zeta(x) \left\{ \Psi_1^\dagger(x) \Psi_3(x) + \Psi_1(x) \Psi_3^\dagger(x) - \Psi_2(x) \Psi_4^\dagger(x) - \Psi_2^\dagger(x) \Psi_4(x) \right\}. \quad (29)$$

Then they disappear in the definition (28). This problem permits an exact solution, since we are left with a quadratic Hamiltonian expressed in terms of the $\Psi_i(x)$

operators. We obtain this solution via the equations of motion

$$(\partial_t \pm \partial_x) \Psi_{1,3}^\dagger(x, t) = \pm \lambda \zeta(x) \Psi_{3,1}^\dagger(x, t) \quad (30)$$

$$(\partial_t \pm \partial_x) \Psi_{2,4}^\dagger(x, t) = \mp \lambda \zeta(x) \Psi_{4,2}^\dagger(x, t). \quad (31)$$

They describe free chiral fermions with linear dispersion outside of the contact area. The contact region, $|x| \leq L_c/2$, then acts as a scatterer. Denoting by $a_i^\dagger(k)$ ($b_i^\dagger(k)$) the momentum-space creation operator for fermions moving towards (away from) the scatterer, their respective particle densities can be related by a transmission matrix $D_{ij}(k)$,

$$\langle : b_j^\dagger(k) b_j(k) : \rangle = \sum_{i=1}^4 D_{ji}(k) \langle : a_i^\dagger(k) a_i(k) : \rangle. \quad (32)$$

The matrix D_{ij} can be found in closed form from Eqs. (30) and (31), see Sec. 3.3.2.

To solve the full transport problem, we also need to re-express the boundary conditions (4) in the new fermion basis. Defining $\rho_i(x) = \langle : \Psi_i^\dagger(x) \Psi_i(x) : \rangle$ as density of the new fermions, for $g = 1/2$, we get the relation to the previous densities $\rho_{p\alpha}(x)$ (where $p = \pm = R/L$):

$$\begin{aligned} \rho_{p1}(x) &= (1 + 2p)[\rho_1(x) + \rho_2(x)] + (1 - 2p)[\rho_3(x) - \rho_4(x)] \\ \rho_{p2}(-x) &= (2p - 1)[\rho_1(x) - \rho_2(x)] - (1 + 2p)[\rho_3(x) + \rho_4(x)]. \end{aligned}$$

The normal ordering should be performed with respect to the ground state, given by a Fermi sea filled up to $k = 2k_{F1}$ and $k = \mp 2k_{F2}$ for channels (1,2) and (3,4), respectively. Plugging these last relations into Eq. (4) gives the boundary conditions:

$$\begin{aligned} 3\rho_1^- + 3\rho_2^- + \rho_3^- - \rho_4^- &= U_1/4\pi, \\ -\rho_1^+ + \rho_2^+ - 3\rho_3^+ - 3\rho_4^+ &= -U_2/4\pi, \\ \rho_1^+ + \rho_2^+ + 3\rho_3^+ - 3\rho_4^+ &= -U_1/4\pi, \\ -3\rho_1^- + 3\rho_2^- - \rho_3^- - \rho_4^- &= U_2/4\pi, \end{aligned} \quad (33)$$

where $\rho_i^\pm = \rho_i(\pm L/2)$. For the current, one gets

$$I_1 = 2[\rho_1(x) + \rho_2(x) - \rho_3(x) + \rho_4(x)]. \quad (34)$$

Here x is arbitrary due to the continuity equation. The incoming free fermions must obey the Fermi distribution,

$$\langle : a_j^\dagger(k) a_j(k) : \rangle = n_F(k - \mu_j) - n_F(k),$$

with $n_F(E) = 1/[\exp(E/T) + 1]$. Therefore we obtain

$$\rho_j^\mp = \int \frac{dk}{2\pi} \langle : a_j^\dagger(k) a_j(k) : \rangle \equiv \mu_j, \quad (35)$$

where $-$ sign should be taken for channels 1 and 2, and $+$ for 3 and 4. The effective chemical potentials μ_j have to be computed self-consistently, see below. The outgoing densities are then given by

$$\rho_j^\pm = \sum_{i=1}^4 \int \frac{dk}{2\pi} D_{ji}(k) [n_F(k - \mu_i) - n_F(k)], \quad (36)$$

where \pm apply to the channels (1,2) and (3,4), respectively.

3.3.2 Transmission matrix

The transmission matrix contains only one independent element. Obviously, $D_{13} = D_{31}$, $D_{11} = D_{33}$, $D_{24} = D_{42}$, and $D_{22} = D_{44}$ because of the system symmetry. All other matrix elements vanish since the channels (1,3) and (2,4) fully decouple. Furthermore, since the Hamiltonian (29) conserves the net particle numbers in channels (1,3) and (2,4), one has the additional relations $D_{13}(k) = 1 - D_{11}(k)$ and $D_{24}(k) = 1 - D_{22}(k)$. The last simplification stems from the symmetry of the equations of motion and reads $D(k) = D_{22}(k) = D_{11}(k)$.

Let us now explain how to find $D(k)$. Since a right-mover in channel 1 is scattered to a left-mover in channel 3 within the contact, we can regard them as a single species which is backscattered by the contact. Then the problem reduces to the determination of the penetration coefficient of 1D fermions through a rectangular barrier. The corresponding result can be found, e.g. in Ref. [19],

$$D(k) = \frac{4k^2|\chi|^2}{\lambda^4|\sin[L_c\chi]|^2 + 4k^2|\chi|^2}, \quad (37)$$

where $\chi^2 = k^2 - \lambda^2$. Next we insert Eqs. (35) and (36) into the boundary conditions (33) and compute the current from Eq. (34).

3.3.3 Linear transconductance

The *linear transconductance* G_{12} can be found in closed form, where we focus on $T = 0$ and $\delta k_F = 0$ again. Notably, this quantity does not vanish in general as it would for a point-like coupling. Linearizing Eq. (36) in the chemical potentials μ_i , we need to solve the now linear system of equations (33) for the μ_i , yielding

$$2G_{12}/G_0 = \frac{1 - D(2k_F)}{1 - D(2k_F)/2}, \quad (38)$$

For uncoupled nanotubes, $\lambda \rightarrow 0$, we find $D(2k_F) = 1$ and thus $G_{12} = 0$. On the other hand, for strongly coupled tubes, $\lambda \rightarrow \infty$, we get $D(2k_F) = 0$ and hence recover the absolute Coulomb drag, $G_{12} = e^2/2h$, in this limit. For small contact lengths, it is possible to perform a Taylor expansion of $D(k)$. The resulting linear transconductance behaves according to

$$2G_{12}/G_0 = \frac{1}{8}(\lambda L_c)^2 (\lambda/k_F)^2. \quad (39)$$

The local approach of Section 3.2 for $g = 1/2$ gives

$$2G_{12}/G_0 = \frac{1}{3}(2\pi V_{1b} L_c)^2 (k_F L_c)^2, \quad (40)$$

where V_{1b} denotes the coupling strength of the related local problem, see Eq. (21). These two results suggest the following relation between the coupling constants

$$V_{1b} = \frac{1}{4\pi a} \left(\frac{3}{2}\right)^{1/2} \left(\frac{\lambda}{k_F}\right)^2 \frac{1}{L_c}, \quad (41)$$

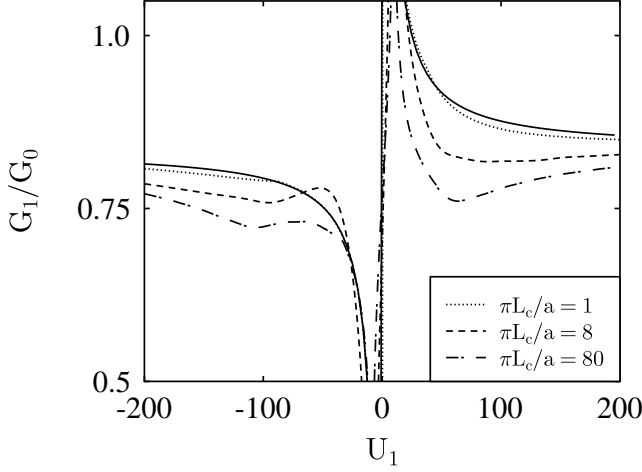


Fig. 4. Nonlinear conductance G_1 (in units of $G_0 = e^2/h$) as a function of U_1 for $g = 1/2$, $T = 0$, $\lambda = 4$, $U_2 = 25$, and various contact lengths. The solid curve is obtained analytically for the shortest contact using the point-like coupling (13).

which establishes a connection between the local approximation and the exact solution for the system with a short contact. The corresponding amplitudes V_{1b}^\pm are then given by a Taylor expansion of Eqs. (21) to second order in L_c/a , implying that $V_{1b}^- = V_{1b}$ and $V_{1b}^+ = V_{1b}(1 - 2(k_F L_c)^2/3)$.

Moreover, employing the Sommerfeld expansion, the finite-temperature corrections

$$\Delta G_{12}(T) = G_{12}(T) - G_{12}(T = 0)$$

to Eq. (38) are of the form

$$\Delta G_{12}(T)/G_0 = -\frac{\pi^2 T^2}{6} \frac{\partial^2 D(k = 2k_F)}{\partial k^2} \frac{1}{(2 - D(2k_F))^2}$$

In the general nonlinear case, the current has to be evaluated numerically, see Fig. 4. All curves show a singularity at $U_1 \rightarrow 0$, independent of L_c . This singularity implies non-vanishing current for zero applied voltage and reflects Coulomb drag.

3.3.4 Absolute Coulomb drag

The absolute Coulomb drag reported in Refs. [8,9] can be recovered by our $g = 1/2$ solution. For a very long contact ($L_c = L$), H can be diagonalized by means of a Bogoliubov transformation. Consider, e.g. channels $j = 1$ and 3, with

$$\Psi_j(x) = \int \frac{dk}{2\pi} e^{ikx} c_j(k).$$

Allowing for $\delta k_F \neq 0$ and switching to

$$\begin{aligned} \alpha_1(k) &= c_1(k) \cos \delta_k + i c_3(k) \sin \delta_k, \\ \alpha_3(k) &= -c_1(k) \sin \delta_k + i c_3(k) \cos \delta_k, \end{aligned}$$

where $2\delta_k = \arctan(\lambda/(k + \delta k_F))$, we find for the channels 1 and 3:

$$\begin{aligned} H_{1,3} &= \int \frac{dk}{2\pi} \left[2k_F + \sqrt{(k + \delta k_F)^2 + \lambda^2} \right] \alpha_1^\dagger(k) \alpha_1(k) \\ &\quad + \left[2k_F - \sqrt{(k + \delta k_F)^2 + \lambda^2} \right] \alpha_3^\dagger(k) \alpha_3(k). \end{aligned}$$

The Hamiltonian $H_{2,4}$ follows accordingly by replacing $\delta k_F \leftrightarrow 2k_F$.

We can now distinguish two situations: (i) $|\delta k_F| \ll \lambda$, where the channels $j = 1, 3$ are gapped and therefore transport for $U_{1,2} \ll \lambda$ is strongly suppressed, and (ii) $|\delta k_F| \geq \lambda$, with no gap. Since $k_F \gg \lambda$, transport properties involving the channels 2 and 4 will always be perfect. For case (ii), the coupling λ will thus not significantly affect transport, i. e. up to weak perturbations, the quantized ideal currents are found. However, for case (i), we obtain at $T = 0$

$$I_1 = (e^2/2h)(U_1 + U_2), \quad (42)$$

just as is expected for absolute Coulomb drag. This simple calculation shows that sufficiently large δk_F can destroy the perfect Coulomb drag. Experimentally, this could be achieved by uniformly shifting the chemical potentials of the two reservoirs attached to the same wire.

4 Weakly coupled reservoirs

How important is the requirement of good (adiabatic) contact to the reservoirs assumed in our theory so far? Is it still possible to observe the characteristic effects of crossed LL transport and Coulomb drag with weakly coupled reservoirs? To study this point, we assume now that reservoirs are coupled to the QWs by tunnel junctions with (identical) dimensionless tunnel conductance $T_0 \ll 1$. In this section, we consider only the limit of zero temperature and sufficiently large applied voltage such that transport proceeds incoherently at all contacts.

The applied voltage U_1 will then split up into three voltage drops: First, the part U_1' drops at each junction, and U_1'' at the contact between the nanotubes, where $U_1 = 2U_1' + U_1''$. The current I_1 injected into the QW from the (say, left) reservoir is then

$$I_1 = T_0 G_0 U_1' |a U_1'|^{\nu_g - 1}. \quad (43)$$

Here the exponent $\nu_g = 1/g$ applies to the case of an end-contacted (spinless single-channel) QW, while $\nu_g = (g + 1/g)/2$ for a bulk-contacted QW [3]. If the voltage drop U_1'' across the crossing point is significantly higher than U_1' , the correlation effects described in the previous section dominate the transport process, and we may use the strong-coupling form of the current [4],

$$I_1 = G_0 T_B \sum_{\pm} \text{sgn}(U_1'' \pm U_2'') (|U_1'' \pm U_2''|/T_B)^{1/g-1}. \quad (44)$$

Since both Eq. (43) and (44) must give the same current, the condition $U_1'' \gg U_1'$ leads to the estimate

$$U_1, U_2 \gg T_B [T_0 (a T_B)^{\nu_g - 1}]^{-1/(\nu_g + 1 - 1/g)}. \quad (45)$$

Once this condition is satisfied, typical crossed LL effects can be observed even for non-adiabatic (weak) coupling to the voltage reservoirs. Evidently, Eq. (45) cannot be satisfied for end-contacted QWs. This is because the power-law exponent in Eq. (45) is always negative (namely -1), and with $T_0 \ll 1$ the inequality cannot be satisfied except for unreasonably high U_1 . However, assuming that we have *bulk-contacted* QWs with $g < \sqrt{2} - 1 \simeq 0.414$, the power-law exponent changes sign, and then the condition (45) can be fulfilled even for very small applied voltage U_1 .

5 Electron tunneling

Let us now address the influence of electron tunneling between the QWs. For clarity, we shall focus on the case of a strict point-like contact ($L_c \rightarrow 0$) as in Sec. 3.1. Assuming $g < 1$, tunneling is then irrelevant under the RG and can be treated to lowest order in the tunneling matrix element t (unless t is very large). In addition, we restrict ourselves to small applied voltages, $|U_{1,2}|, \delta k_F \ll T_B$, at zero temperature, where the tunneling density of states (TDOS) describing electron tunneling into QW $\alpha = 1, 2$ (at $x = 0$) in the presence of the electrostatic coupling carries the standard power-law suppression factor [14]

$$\rho(E) \propto \Theta(E)E^{1/g-1}. \quad (46)$$

Of particular interest will be the effect of $\delta k_F = k_{F1} - k_{F2}$ on the transport properties in the presence of tunneling (without loss of generality, we consider $\delta k_F > 0$).

Tunneling modifies the currents flowing to the left and to the right of the coupling point $x = 0$. Under a golden rule calculation, these currents can be easily found from the rates for tunneling of a $p = \pm = R/L$ mover in QW 1 into a p' mover in wire 2:

$$\Gamma_{p1 \rightarrow p'2} = |t|^2 \Theta(\Delta_{pp'}) \int_0^{\Delta_{pp'}} dE \rho(E) \rho(\Delta_{pp'} - E). \quad (47)$$

Because of the pointlike coupling, there is no momentum conservation, and the tunneling electron can change its chirality. In Eq. (47),

$$\Delta_{pp'} = \delta k_F / g + \mu_{p1} - \mu_{p'2}, \quad (48)$$

where $\mu_{p\alpha}$ is the chemical potential of a p mover in QW $\alpha = 1, 2$ (relative to the respective mean chemical potential), which is determined by the applied voltages $U_{1,2}$ and the electrostatic coupling T_B . Simple dimensional scaling gives from Eq. (47)

$$\Gamma_{p1 \rightarrow p'2} \propto \Delta_{pp'}^{2/g-1}. \quad (49)$$

For $\delta k_F \gg g|U_1, U_2|$, the tunneling rates become independent of the applied voltages $U_{1,2}$. In this limit, tunneling rates are large, and therefore tunneling can potentially modify the transport behaviors discussed in Sec. 3. However, for $\delta k_F \ll g|U_1, U_2|$, the rates are power-law suppressed, and hence tunneling rates become very small. In

fact, since the power-law exponent is larger than the one in the absence of tunneling, see Eq. (44), we expect that tunneling leads only to *subleading* corrections for small δk_F . The role of tunneling in a concrete experiment could then be revealed by simply tuning δk_F from zero to large values. If this leads to a destruction of the crossed LL scenario, tunneling matrix elements must be sizeable and should be taken into account for large δk_F .

6 Conclusions and applications

Let us briefly summarize the conclusions and major findings of our paper. We have studied transport through two quantum wires or carbon nanotubes that are coupled along a contact length L_c . Assuming that the wires are in the Luttinger liquid state with sufficiently strong interactions, the main coupling mechanism is of electrostatic nature, and tunneling provides only perturbative corrections to the problem. The electrostatic coupling leads to qualitatively new nonequilibrium transport behaviors compared to the case of Fermi liquid wires, namely crossed Luttinger liquid effects and Coulomb drag. Crossed Luttinger liquid effects are characterized by pronounced zero bias anomalies, dependencies of transport currents on applied cross voltages, and resonant behaviors at finite voltages. For extended contacts, very pronounced Coulomb drag effects arising at low temperatures were found. For short contacts, the linear transconductance has a maximum at a finite temperature and approaches zero as $T \rightarrow 0$.

For sufficiently long contacts Coulomb drag can even be perfect at low temperatures, with the transconductance approaching its largest possible value $e^2/2h$. We have presented an exact solution of the full transport problem valid for arbitrary contact length L_c at the special interaction strength $g = 1/2$. In addition, the nonlinear properties of Coulomb drag and their relation to crossed Luttinger liquid effects were clarified. Our study has assumed adiabatic coupling to the voltage reservoirs. However, as outlined in Sec. 4, for sufficiently strong interactions, the same characteristic effects are expected for bulk-contacted nanotubes, where the nanotubes are in weak (tunneling) contact with the leads. In addition, we have shown that the tunneling between the nanotubes should cause only subleading corrections to the behaviors outlined here for small $\delta k_F = k_{F1} - k_{F2}$. However, by varying this quantity, the role of tunneling can be easily determined in practice. For large δk_F , the characteristic correlation effects will be washed out by a sufficiently large tunneling matrix element.

Let us conclude the paper with two possible applications. Crossed nanotubes could be used for *voltage amplification*, e.g. by using the circuit shown in Fig. 5. The circuit equation $U_1[1 + RG(U_1, U_2)] = U_0$ can be easily solved for $g = 1/4$ and $T = 0$, with the results depicted in Fig. 6. Clearly, the voltage amplification ratio $\partial U_2 / \partial U_1$ can be tuned to extremely high values. A more complex setup built up of three nanotubes coupled to each other in a star-like manner is shown in Fig. 7. If the distance L_K between the contact points exceeds the length scales v/T

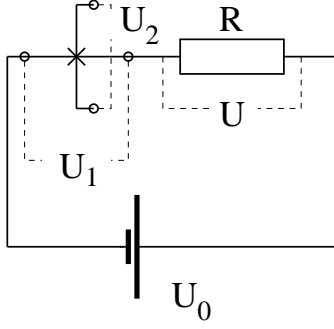


Fig. 5. Amplification circuit based on crossed nanotubes. For fixed R and U_0 it is possible to achieve $|\partial U_2 / \partial U_1| \gg 1$.

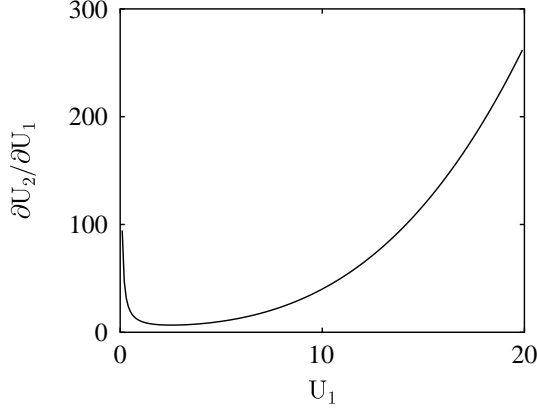


Fig. 6. Voltage amplification ratio for $RG_0 = 1$ at $T = 0$ and $g = 1/4$ (here $T_B = 1$).

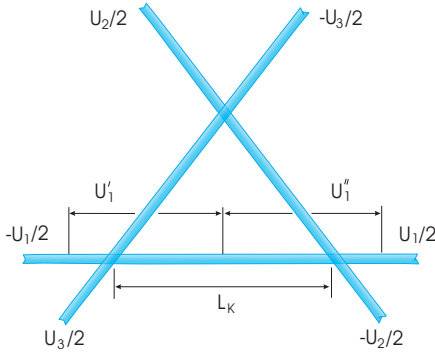


Fig. 7. Triangular setup of nanotubes coupled by (local) electrostatic interactions.

or v/U_i , transport proceeds in an incoherent way and can thus be modelled as a sequence of crossed LLs. The voltage drops U'_i and U''_i arising at the respective contacts obey $U_i = U'_i + U''_i$, and now effectively play the role of two-terminal voltages. This allows for the direct application of the results of Sec. 3, and the whole current-voltage characteristics of such a setup can be obtained. We only point to one interesting consequence of this solution, namely the possibility of a *voltage measurement* involving only elec-

trostatic contact. Setting, say, $U_3 = 0$, the current I_1 is seen to vanish once $U_1 = -\kappa U_2$, where κ is constant and assumed to be known from previous measurements. The (presumably unknown) voltage U_2 can thus be determined by tuning U_1 to the point where $I_1 = 0$.

We thank A. O. Gogolin and H. Grabert for discussions, and the Deutsche Forschungsgemeinschaft for support under Grant No. GR 638/19-1 and the Gerhard-Hess program.

References

1. A. O. Gogolin, A. A. Nersesyan and A. M. Tsvelik, *Bosonization and Strongly Correlated Systems* (Cambridge University Press 1998).
2. M. Bockrath, D. H. Cobden, J. Lu, A. G. Rinzler, R. E. Smalley, L. Balents, and P. L. McEuen, *Nature* **397**, 598 (1999); Z. Yao, H. Postma, L. Balents, and C. Dekker, *ibid.* **402**, 273 (1999).
3. R. Egger and A. O. Gogolin, *Phys. Rev. Lett.* **79**, 5082 (1997); *Eur. Phys. J B* **3**, 281 (1998); C. Kane, L. Balents, and M. P. A. Fisher, *Phys. Rev. Lett.* **79**, 5086 (1997).
4. A. Komnik and R. Egger, *Phys. Rev. Lett.* **80**, 2881 (1998).
5. J. Kim, K. Kang, J.-O. Lee, K.-H. Yoo, J.-R. Kim, J. W. Park, H. M. So, and J.-J. Kim, preprint cond-mat/0005083.
6. A. G. Rojo, *J. Phys. Cond. Mat.* **11**, R31 (1999).
7. M. S. Fuhrer, J. Nygard, L. Shih, M. Forero, Y.-G. Yoon, M. S. C. Mazzoni, H. J. Choi, J. Ihm, S. G. Louie, A. Zettl, and P. McEuen, *Science* **288**, 494 (2000); H. Postma, M. de Jonge, Z. Yao, and C. Dekker, preprint.
8. K. Flensberg, *Phys. Rev. Lett.* **81**, 184 (1998).
9. Yu. Nazarov and D. Averin, *Phys. Rev. Lett.* **81**, 653 (1998).
10. R. Klesse and A. Stern, preprint cond-mat/9912371.
11. V. V. Ponomarenko and D. V. Averin, preprint cond-mat/0003118.
12. R. Egger and H. Grabert, *Phys. Rev. Lett.* **77**, 538 (1996); *ibid.* **80**, 2255(E) (1998).
13. O. A. Starykh, D. L. Maslov, W. Häusler, and L. I. Glazman, *Interactions and Transport Properties of Lower Dimensional Systems* (Springer Lecture Notes in Physics, 2000).
14. C. L. Kane and M. P. A. Fischer, *Phys. Rev. B* **46**, 15233 (1992).
15. R. Egger, H. Grabert, A. Koutouza, H. Saleur, and F. Siano, *Phys. Rev. Lett.* **84**, 3682 (2000).
16. F. V. Kusmartsev, A. Luther, and A. A. Nersesyan, *JETP Lett.* **55**, 724 (1992).
17. V. M. Yakovenko, *JETP Lett.* **56**, 510 (1992).
18. A. Luther and V. Emery, *Phys. Rev. Lett.* **33**, 589 (1974).
19. L. D. Landau and E. M. Lifshits, *Quantum Mechanics*, (Pergamon Press, Oxford, 1982).